Science of the Total Environment 826 (2022) 154144

Contents lists available at ScienceDirect

Science of the Total Environment

journal homepage: www.elsevier.com/locate/scitotenv

Selective sorption and desorption of DOM in podzol horizons — FTIR and Py-GC/MS of leachates from a column experiment

Sara Ramos dos Santos [a], Judith Schellekens [a,b,*], Wilson Tadeu Lopes da Silva [c], Peter Buurman [d], Alexys Giorgia Friol Boim [a], Pablo Vidal-Torrado [a]

[a] Soil Science Department, Luiz de Queiroz Agricultural College - University of São Paulo (ESALQ-USP), Av. Pádua Dias, 11, Piracicaba, SP, Brazil
[b] Department of Earth and Environmental Sciences, KU Leuven, Celestijnenlaan 200E, Leuven, Belgium
[c] Brazilian Agricultural Research Corporation - EMBRAPA Instrumentation Center, R. 15 de Novembro, 1452 São Carlos, SP, Brazil
[d] Water Systems and Global Change Group, Wageningen University, P.O. Box 47, 6700 AA Wageningen, the Netherlands

HIGHLIGHTS

- Column experiment simulating podzolization to study selective retention of DOM
- DOM and its leachates after (de)sorption analyzed with FTIR and Pyrolysis-GC/MS
- Sorption was selective and selectivity depended on DOM type and Al species
- Selective retention of compounds from biomacromolecules
- (De)sorption of DOM-Al complexed by phenolic and carboxylic groups and LMW products

GRAPHICAL ABSTRACT

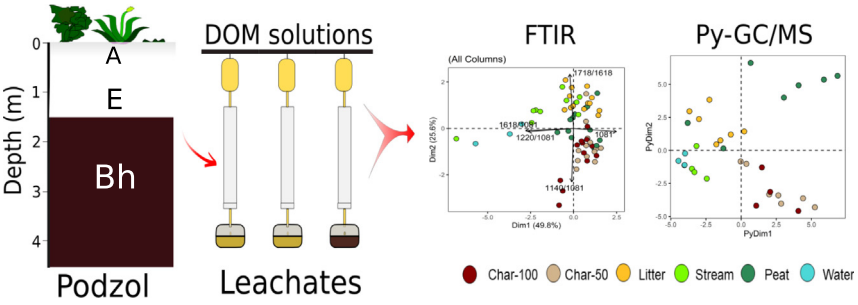

ARTICLE INFO

Article history:
Received 29 November 2021
Received in revised form 18 February 2022
Accepted 21 February 2022
Available online 25 February 2022

Editor: Jay Gan

Keywords:
Podzolization
Tropical coastal podzols
Natural organic matter
DOM-metal binding properties
Desorption
Experimental pedology

ABSTRACT

The sorption of dissolved organic matter (DOM) depends on its interaction with the soil matrix. In hydromorphic podzols, DOM reacts mainly with aluminium (Al), which is responsible for the formation of the Bh-horizon in the subsoil. In this work, we investigated whether the retention of DOM in the soil during the podzolization process is selective in relation to the molecular composition of DOM. A column experiment was conducted to study the selective retention of sorption and desorption processes under controlled conditions. Materials used in the column experiment were representative for Brazilian coastal podzols under tropical rainforest. Materials were collected from this tropical coastal podzol ecosystem, and included soil from E- and Bh-horizons, and DOM from a stream (Stream), peat water (Peat), litter (Litter) and charred litter (Char). To evaluate selective retention of DOM, both the initial DOM and its leachates were analyzed by Fourier transform infrared spectra absorption (FTIR) and pyrolysis gas-chromatography/mass spectrometry (Py-GC/MS). The results showed preferential retention of DOM associated with biopolymers for soil columns with E-horizon material (E), E with Al nitrate (E-n), E with kaolinite (E-k) and E with gibbsite (E-h), except for Char. The composition of leachates after percolation through B horizon columns was mainly determined by desorption, and had a relatively large contribution from phenolic and carboxylic groups associated with Al and low molecular weight aromatic and N-containing pyrolysis products, while products from macromolecular materials such as cellulose were selectively retained in the columns for all DOM types. DOM from the Stream (taken during the rainy season) resembled that of desorbed OM from the B columns, reinforcing substantial desorption in the field as well. Our results suggest that sorption and desorption of OM in the hydromorphic Bh-horizon is continuous and that the selectivity of sorption is dependent on DOM source.

* Corresponding author at: Soil Science Department, Luiz de Queiroz Agricultural College - University of São Paulo (ESALQ-USP), Av. Pádua Dias 11, Piracicaba, SP, Brazil.
E-mail address: schellekens.j@hetnet.nl (J. Schellekens).

http://dx.doi.org/10.1016/j.scitotenv.2022.154144

1. Introduction

Dissolved organic matter (DOM) can be retained in the soil through sorption on mineral surfaces and/or (co)precipitation with metals such as aluminium (Al) (Guggenberger and Kaiser, 2003; Jansen et al., 2003; Zhang et al., 2021). The mobility and solubility of DOM in the soil environment makes it the most active organic matter (OM) fraction in terms of its binding properties with metals and minerals (Nierop et al., 2002). Understanding the DOM-Al binding mechanisms is important in environmental biogeochemistry studies, such as transport of contaminants and the retention and stability of soil OM (SOM) (Kaiser and Guggenberger, 2000; Kalbitz et al., 2005; Scheel et al., 2007). To predict the dynamics of DOM in the soil it is essential to know whether some DOM compounds are preferentially bound to metals and/or mineral surfaces (Kalbitz et al., 2005; Scott and Rothstein, 2014). Also, successful management of environmental problems requires an understanding of the mechanism behind selectivity in sorption processes such as complexation, ligand exchange, cation bridges, anion/cation exchange, van der Waals interactions, and hydrophobic bonding (Guggenberger and Kaiser, 2003; Zhang et al., 2021).

In terrestrial ecosystems, DOM can be derived from plants, litter, root exudates, microbial metabolites and charcoal, and may be present at various stages of decomposition (Nebbioso and Piccolo, 2013). DOM degradation is controlled by environmental factors, intrinsic properties of the source material, and protection by the mineral phase (Mikutta et al., 2007; Kiikkilä et al., 2012). Thus, the composition of DOM may be highly variable and depends on its history. Because the reactivity and solubility of DOM are controlled by its molecular composition (i.e., molecular size, and functional groups; Kothawala et al., 2012), changes in DOM composition can affect the interaction with metals and minerals (Boča et al., 2020).

Usually, DOM from litter was used in experiments of binding mechanisms in soils (Zysset and Berggren, 2001; Boča et al., 2020), and it has been found that aromatic compounds with carboxylic and phenolic functional groups bind preferentially. This is related to the ligand exchange reactions of these functional groups that form inner sphere complexes with clay and metal oxides (Kaiser et al., 1997; Kaiser and Guggenberger, 2000; Guan et al., 2006; Avneri-Katz et al., 2017).

Podzols represent a natural environment in which the interaction between metals and OM is the key process. Understanding mobilization and immobilization of DOM in these soils may improve the comprehension of soil genesis and biogeochemistry (Zysset and Berggren, 2001, Jansen et al., 2005; Harris and Rischar, 2012; Lopes-Mazzetto et al., 2018a). DOM from vertical and/or lateral flow may precipitate with Al and/or Fe in the subsurface where it forms the podzol B-horizon. In poorly drained podzols, Fe is leached through groundwater flow, and the OM in the B-horizon exclusively has a DOM source, while in well-drained podzols Fe can be present (depending on the parent material) and B-horizon OM has a large contribution from roots as well (De Coninck, 1980; Buurman and Jongmans, 2005). In tropical coastal areas, poorly drained podzols are abundant and often have a thick and well-developed B-horizon (Martinez et al., 2018; Lopes-Mazzetto et al., 2018a). Therefore, poorly drained tropical podzols are natural and unique laboratories to study DOM-Al binding mechanisms.

The aim of this study was to test whether retention of DOM in the soil is selective. To this end, the interaction of several DOM-types with different materials was tested under controlled conditions in a column experiment. We compared the composition of DOM before and after percolation through soil columns. DOM composition was analyzed by functional groups (FTIR) and molecular structure (Py-GC/MS). Our hypotheses are: i) the interaction of DOM with Al species in the columns is selective, and ii) retention of DOM without the addition of Al also occurs and is not selective. Additionally, it was tested whether DOM precipitated in a podzol B-horizon could be released by percolation with DOM solutions or water, and whether such a release was also selective.

2. Material and methods

2.1. Sampling, and characteristics of column materials and DOM

The materials used in the column experiment were from podzol E- and B-horizons collected on the barrier island of Ilha Comprida (State of São Paulo, Brazil). The area formed by sandy coastal sediments is part of a *Restinga* ecosystem. *Restinga* is composed of tropical rainforest vegetation that is adapted to oligotrophic sandy soils, and is typically composed of trees of several sizes, palms, grasses, bromeliads, and shrubs (Leão and Dominguez, 2000). The sampled tropical coastal podzol, located in the south cliff (Ponta da Trincheira 23 J 0206148 W 7226166 S; SI_Fig. 1) was classified as an Ortstenic Albic Podzol (Arenic, Hyperspodic). The sampled podzol is hydromorphic, indicated by the flat and abrupt transition between the E- and B-horizon, very thick B-horizon and absence of Fe in the podzol B-horizon (Bh) (Buurman and Jongmans, 2005). Material from the E- and B-horizon was collected at depths of 100–150 cm and 180–320 cm, respectively. The E-horizon had 0.13% of total organic carbon (TOC), 0.01% of Al extracted by sodium pyrophosphate ($Na_4P_2O_7.10H_2O$; 0.1 mol L^{-1}) at pH = 10, and 1.3% clay. The Bh-horizon had an average of 0.75% of TOC, 0.06% of Al extracted by sodium pyrophosphate, and 2% clay (Martinez et al., 2018).

Four different DOM solutions were used: 1) from a little stream near a rainfall station (Stream), 2) peat water (Peat), 3) a solution of litter (Litter), and 4) a solution of charred litter (Char). These DOM types are selected to represent the most diverse DOM sources that may infiltrate with percolating water and/or via lateral (groundwater) flow into the soils from the study area (SI_Fig. 1). The (charred) litter solutions were prepared in the laboratory. Both the stream and peat are located in the *Restinga* forest. Water from the stream was sampled in the wet season in February 2018 (23 J 0206269 W 7226113 S) and water from the peat was sampled during the dry season (September 2018; 23 J 02078706 W 7226956 S). The char and litter samples were collected from burnt and unburnt spots in the surroundings of the podzol profile, and were dried for 2–3 days at 40 °C, and ground (<2 mm) to prepare DOM solutions. For DOM from litter and charred material, 100 g of each material was added to 1 L of deionized water and shaken for 24 h at 180 rpm, centrifuged, and passed through a 0.7 μm glass fiber membrane (Refaey et al., 2014). Aqueous samples from both streams were filtered through a 0.7 μm glass fiber membrane and stored at 4 °C. All DOM solutions were brought to a DOC concentration and pH similar to that of Stream (54 mg L^{-1}, pH = 4), to allow comparison of the different DOM types at similar conditions. Additionally, a double DOC concentration for the char was used (117 mg L^{-1}). Because the B-horizon naturally contains SOM, distilled water was used as a reference for desorption in the columns with B-horizon material.

2.2. Experimental design

An overview of columns and percolating solutions is given in SI_Table 1 and Fig. 1. PVC pipes with a diameter of 5 cm and a height of 35 cm were filled with soil material to a height of 30 cm. PVC caps with a plastic hose fixed to a central hole were attached to the bottom of the columns. A layer of fiberglass filter was placed inside of each column to avoid material loss and clogging of the collector hoses. All the columns were placed on a wooden support in an upright position (Fig. 1). The B-horizon material was dried at 40 °C for 48 h. All E-horizon material were calcined at 900 °C for 4 h to remove OM (Sutherland, 1998). The chosen Al sources were kaolinite ($Al_2Si_2O_5(OH)_4$), gibbsite ($Al(OH)_3$), and Al nitrate ($Al(NO_3)_3.9H_2O$). The E-horizon material contained very low amounts of TOC, Al, and clay.

The columns with E-horizon material without added Al source were used as a reference for retention of DOM in the column (E). To measure the effect of clay, columns were filled with a mixture of E-horizon material with 1% kaolinite (E-k). Kaolinite is a common clay mineral in tropical coastal podzols (Gomes et al., 2007). The kaolinite has a particle-size distribution of 20.5% clay, 52.8% silt and 26.7% sand, 0.18% TOC, dried at 105

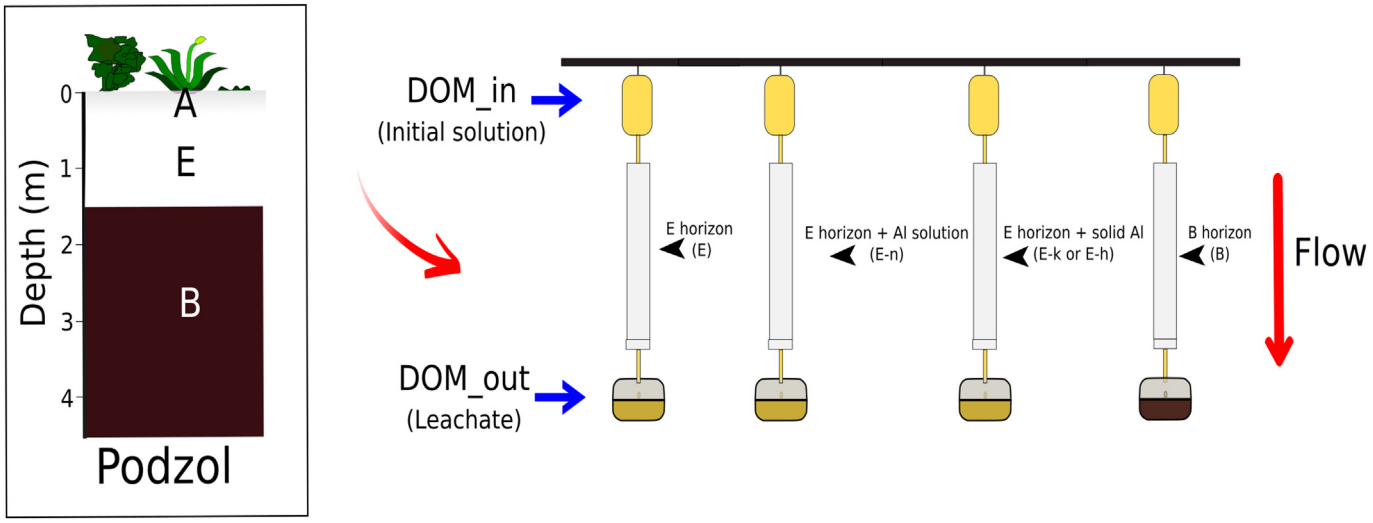

Fig. 1. Schematic overview of the column experiment, and illustration of the column materials used.

°C). Similar to E-k, 1% of gibbsite was used for the columns filled with a mixture of E-horizon material and gibbsite (E-h). To measure the effect of readily available Al^{3+} and optimize precipitation (Martin and Reeve, 1961; Jansen et al., 2003), columns of E-horizon material were also saturated with a solution of 3.4 10^{-3} mol L^{-1} Al nitrate (E-n).

For E-k and E-h columns, the amount of 1% (*w*/w) of kaolinite or gibbsite was mixed thoroughly with the E-horizon material before being inserted into the column. Then, deionized water (approximately 15% of its maximum saturation point) was added to all samples to make them more friable and homogeneous. The samples were packed into the column in layers of 100 cm^3, making light compactions to each one. This procedure aimed to reduce the differences between the experimental plots, ensuring more regular soil density in the columns and avoiding bypass flow (Pavinato et al., 2018). After this process, all columns were saturated with distilled water until 70% of the field capacity, which was 227 and 262 mL for E- and B-horizon material, respectively) to regulate the water flux.

For the experiment 2 L of DOM solution was used, except for the Stream (0.5 L; SI_Table 1). The flow was controlled using surgical needles with a diameter of 0.45 mm, adapted to an average flow rate of 20 mL h^{-1} (Refaey et al., 2014), and resulting in a total reaction time of four to five days. The leachates after passing through the column were collected in pots of 500 mL. All treatments were carried out in triplicate resulting in a total of 63 columns (SI_Table 1). Original DOM solutions (DOM_in) and leachates (DOM_out) were freeze-dried and homogenized with an agate mortar, resulting in 68 DOM samples for analyses.

2.3. FTIR analyses

The infrared absorption FTIR spectra of homogenized DOM samples were obtained by a Bruker model Vertex 70 FT-IR at Embrapa Instrumentação (São Carlos – Brazil). Analyses were carried-out in triplicate, in a standard region range from 4000 to 400 cm^{-1} with a 4 cm^{-1} resolution and 32 scans per sample. The spectra were obtained from homogenized samples on KBr pellets (IR spectroscopic Degree, Sigma Aldrich) (Capriel et al., 1995; Celi et al., 1997; Ellerbrock and Kaiser, 2005). The proportion for KBr and freeze-dried DOM material was 1:400 and for column materials 1:200 and the mixtures were pressed into pellets. Baseline correction of the spectra was done using Multiplicative Scattering Correction. Infrared bands were assigned according to the main organic bands and their corresponding inorganic functional groups presented in SI_Table 2 and organic functional groups in SI_Table 3.

2.4. Py-GC/MS

Pyrolysis was performed at the Department of Soil Science from ESALQ/USP (Piracicaba, Brazil) using a single shot PY-3030S pyrolyzer (Frontier Laboratories, Fukushima, Japan) coupled to a GCMS-QP2010 (Shimadzu, Kyoto, Japan). The pyrolysis temperature was set at 600 °C (±0.1 °C). Helium was used as carrier gas at a constant flow of 34.5 mL min^{-1}. The injection temperature of the GC (split 1:20) and the GC/MS interface were set at 320 °C. The GC oven was heated from 50 to 320 °C (held 10 min) at 7 °C min^{-1}. The GC instrument was equipped with an UltraAlloy-5column, length 30 m, thickness 0.25 mm, diameter 0.25 μm. The MS was scanning in the range of *m/z* 45–600. Pyrolysis products were identified using the NIST '14 mass spectral library.

The 123 dominant pyrolysis products for the chromatograms of each DOM type were identified and quantified for all samples. Quantification was based on the peak area of characteristic fragment ions (*m/z*) for each product (Table 1). The relative proportion of each product was expressed as a percentage of the total peak area quantified (set at 100%). Quantified products were grouped according to chemical similarity and their source into: lignin phenols, phenols, benzenes, polycyclic aromatic hydrocarbons (PAHs), benzofurans, *n*-alkanes, *n*-alkenes, carbohydrates, and triterpenoids (Table 1). The char samples showed a large peak of dimethylsulfide (*m/z* 48 and 64); with an abundance of >50% it was excluded from the quantification to better compare their composition with the other DOM types. The results of DOM leachates from E-n columns were not quantified because the pyrograms were of poor quality, probably due to interactions between OM and Al and/or nitrate during the pyrolysis process.

2.5. Statistical analysis

Principal component analysis (PCA) was applied separately for FTIR and pyrolysis data, using all DOM_in and DOM_out samples. PCA analysis was used as a statistic tool to reduce dimensions and to identify the reasons for differences among DOM-types and column materials through the quantitative behavior of selected FTIR bands and pyrolysis products. PCA statistical analysis was performed using the prcomp function of R software (Core Team, 2015). Prior to the PCA of pyrolysis results some products were grouped to a single variable using their sum. This grouping was done for products that were highly correlated and in addition have a similar chemical structure. This reduced the number of pyrolysis products to 60 variables. Products that were grouped included 5 guaiacyl lignins (G), 5 syringyl lignins (S), 22 *n*-alkanes

Table 1
Quantified pyrolysis products and their characteristic fragment ions used for quantification[a].

Code[a]	Pyrolysis product	*m/z*	MW	Retention time
B1	Benzene	78	78	2.105
B2	Toluene	91, 92	92	2.792
B3–B5	C_2 Benzenes	91, 106	106	3.942–4.425
B6–B7	C_3 Benzenes	105, 120	120	6.208–6.775
B8–B9	C_4 Benzenes	119, 134	134	6.792–8.042
B10	Benzoic acid	77, 105	122	10.617
B11	Benzenedicarboxylic acid	76, 104	166	13.283
B12	C_3 (1,2-propadienyl)benzene	143, 158	158	13.800
B13–B14	Unidentified benzene compounds	173, 188	188	15.976–16.933
PA1	Naphthalene	128	128	10.142
PA2–PA3	C_1 Naphthalenes	141, 142	142	12.408–12.700
PA4–PA5	C_3 Naphthalenes	155, 170	170	17.250–17.692
PA6	Biphenyl	154	154	13.95
PA7	Fluorene	165, 166	166	17.683
PA8	Phenanthrene	178	178	20.333
PA9	Anthracene	178	178	21.033
PA10–PA13	C_4 Naphthalenes	169, 184	184	17.975–20.183
PA14–PA16	C_1 9*H*-fluorenes	165, 180	180	19.554–19.783
PA17	C_1 Naphthalenol	158, 159	159	19.000
PA18	Unidentified PAH	171, 186	186	15.125
PA19	Dimethyl-1-naphthol	157, 172	172	20.3415
PA20	Unidentified PAH	183, 198	198	20.933
Bf1	Benzofuran	89, 118	118	6.317
Bf2	C_1 Benzofuran	131, 132	132	8.558
Bf3	C_2 Benzofuran	145, 146	146	10.792
Bf4	Dibenzofuran	139, 168	168	16.55
In1	Indene	115, 116	116	7.233
In2	2,3-Dihydro-1*H*-inden-1-one	104, 132	132	12.100
N1	Pyrrole	67	67	2.650
N2	Pyridine	52, 79	79	2.658
N3–N4	C_1 Pyridine	66, 93	93	3.375–4.058
N5–N6	C_1 Pyrrole	80, 81	81	3.675–3.775
N7	Benzonitrile	76, 103	103	6.2165
N8–N9	C_1 Benzoxazoles	133	133	11.0875–12.025
N10	Aminocaproic acid	56, 85	131	11.975
N11	Benzene acetonitrile	90, 117	117	12.567
N12	Unidentified N-containing compound	66, 93		12.683
N13	Unidentified N-containing compound	76, 147		16.025
N14	Diketodipyrrole	93, 186	186	19.858
G1	Guaiacol	109, 124	124	8.142
G2	4-Vinylguaicol	135, 150	150	12.708
G3	4-Acetylguaiacol	151, 166	166	16.025
G4	4-Propan-2-(one)guaiacol	137, 180	180	16.767
G5	Guaiacyl compound	123, 151	151	17.733
S1	Syringol	139, 154	154	13.425
S2	4-Vinylsyringol	165, 180	180	17.300
S3	4-Acetylsyringol	181, 196	196	20.133
S4	4-Propan-2-(one)syringol	167, 210	210	20.692
S5	Syringyl compound	153, 181	181	21.483
Ph1	Phenol	66, 94	94	6.571
Ps1	2-Methylfuran	53, 82	82	3.617
Ps2	2-Methyl-2-cyclopenten-1-one	53, 67	67	4.683
Ps3	2-Acetylfuran	95, 110	110	4.708
Ps4	5-Methyl-2-furaldehyde	109, 110	110	5.667
Ps5	Levoglucosan	60, 73	162	17.642
Ttp1–Ttp2	Unidentified triterpene	191, 231		34.425–35.758
Ttp3	Unidentified triterpene	376		35.625
Ttp4	Unidentified triterpene	215, 344		35.700
Ttp5	Unidentified triterpene	367, 396		36.175
Ttp6	Unidentified triterpene	177, 191		36.233
Ttp7	Unidentified triterpene	191, 205		37.692
Ttp8	Unidentified triterpene	57, 316		40.750
Unk1	Unidentified compound	58, 86		10.867
Unk2	Unidentified compound	112, 157		26.058
Al1-Al3	Aliphatic compounds	55, 71		2.958–3.625
9–31	*n*-Alkanes (C_{9-31})	57, 71		4.483–36.033
9:1–28:1	*n*-Alkenes (C_{9-28})	55, 69		4.358–33.125

[a] Al, Aliphatic; B, Benzene; Bf, Benzofuran; In, Indene; G, Guaiacyl lignin phenols; S, Syringyl lignin phenol; N, N-containing compound; PA, PAH; Ph, Phenol; Ps, Carbohydrate; Ttp, triterpene; Unk, Unidentified compound.

(C:0), 19 *n*-alkenes (C:1), and several groups of isomers (B3–5, B6–7, B8–9, B13–14, PA2–3, PA4–5, PA10–13, PA14–16, N3–4, N5–6, N8–9, Ttp1–2; Table 1).

The selection of FTIR variables is based on the spectra of both column and DOM materials. Peak overlapping with both inorganic and organic bands complicates a quantitative evaluation of the DOM FTIR data.

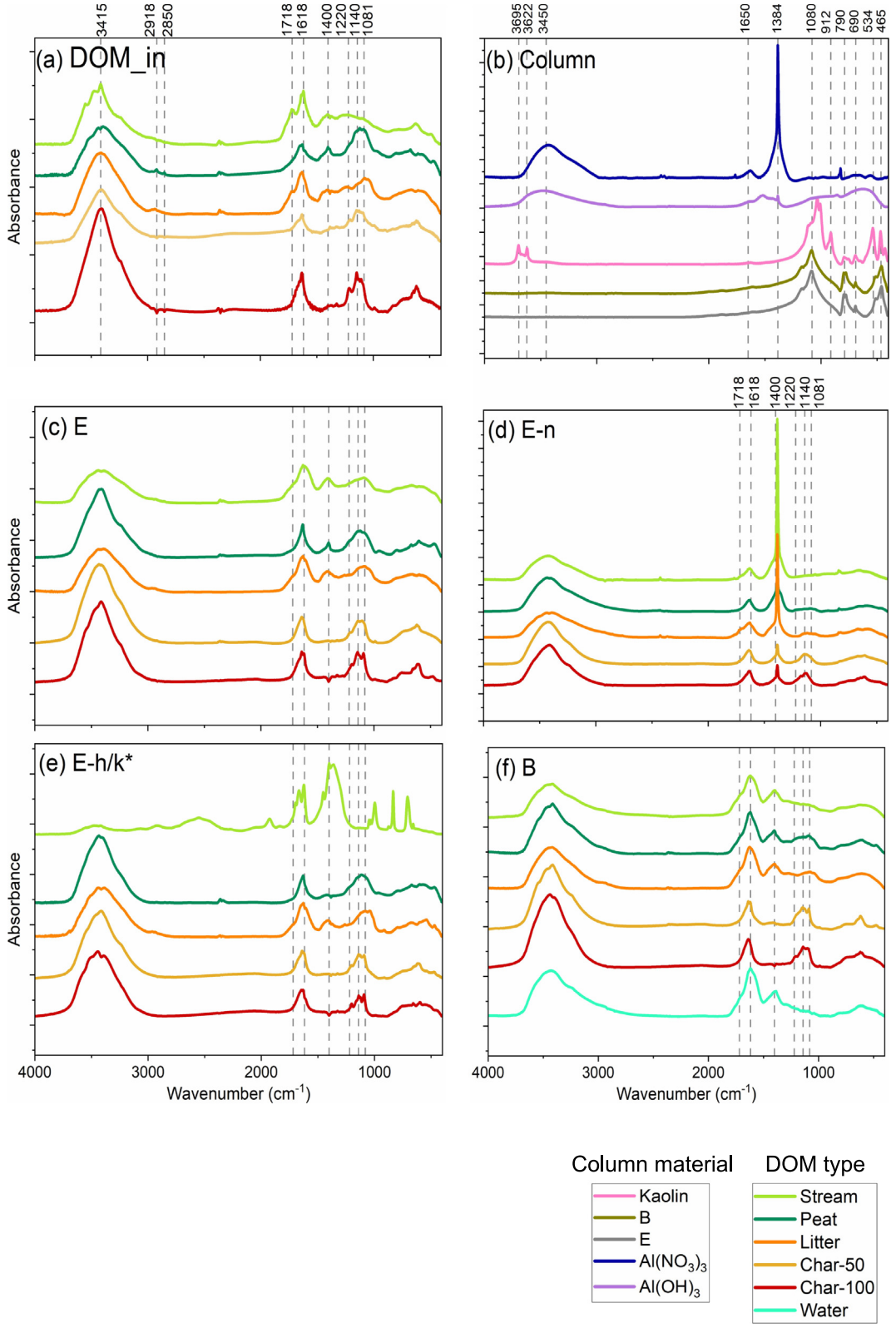

Fig. 2. FTIR spectra from the starting materials of (a) DOM and (b) column materials used in the column experiment, and (c–f) average FTIR spectra of leachates of the different DOM types for each column type ($n = 3$). For the Stream E-h is used instead of E-k.

Quantitative evaluation of organic bands that overlap with inorganic bands cannot be considered for leachates from that column type. To enable interpretation of bands that show overlapping with other organic bands they are expressed as ratios. Detail on the selection of FTIR parameters is provided in Section 3.1.3, based on the results of column materials, initial DOM solutions, and leachates.

3. Results and discussion

3.1. FTIR

3.1.1. Absorption bands of column materials

All column materials were analyzed with FTIR and inorganic bands are presented in Fig. 2b and SI_Table 2. Bands that correspond to silica were present in all column materials (1081, 790, 690, and 465 cm^{-1}, and the two minor shoulders at 1169 and 550 cm^{-1}). This is in line with the dominant presence of quartz grains in these podzol horizons (Lopes-Mazzetto et al., 2018b). The samples from E- and B-horizons presented very similar spectra, which clearly demonstrates the need for SOM purification prior to analysis with FTIR. Bands in the 3700–3600 cm^{-1} region and at 912 and 534 cm^{-1} occurred only in the kaolin sample. These bands correspond to OH stretching and deformation of inner surface hydroxyl groups, and Al-O-Si and SiO deformation, respectively, being indicative of kaolinite (Vaculíková et al., 2011).

The broad bands at the regions of 3450 and 600 cm^{-1} and a minor band at 1650 cm^{-1} were found in $Al(OH)_3$. The broad bands are associated with OH vibrations and stretching vibrations of AlO, respectively; and the minor band is associated to OH bending of sorbed water (Du et al., 2009). The broad bands at 3450 and 1630 cm^{-1} and the sharp bands at 1384 and 830 cm^{-1} were also found in the $Al(NO_3)_3$ spectra; they are associated with OH groups of water (broad bands) and nitrate asymmetric stretch and out-of-plane bend (sharp bands) (Choe et al., 2010).

3.1.2. Composition of the initial DOM solutions

The interpretation of organic absorption bands is given in SI_Table 3. Spectra of the initial DOM solutions are given in Fig. 2a. Bands 3415, 1618, 1220, 1140, and 1081 cm^{-1} were present in all DOM types. The broad hydroxyl band at 3415 cm^{-1} may reflect carboxyl and hydroxyl groups, and is commonly found in SOM and litter (Stevenson and Goh, 1971; Soong et al., 2014). Because the 3415 cm^{-1} band may also reflect water, it is not further discussed (Ellerbrock and Kaiser, 2005).

The 1618 cm^{-1} band from the 1640–1600 cm^{-1} region may represent the carboxylate anion (i.e., deprotonated carboxylic groups: COO^-) (Stevenson and Goh, 1971; Ellerbrock and Kaiser, 2005). The phenolic band at 1220 cm^{-1} is mainly found in lignin moieties (Kaiser et al., 1997; Phinichka and Kaenthong, 2017). The presence of carboxylates (1618 cm^{-1}) and phenols (1220 cm^{-1}) in all DOM spectra is in accordance with the common occurrence of these functional groups in many SOM fractions, and may have a source from plants and microorganisms (Ma et al., 2001).

The 1140 cm^{-1} band can be attributed to aromatic CH and may indicate hydrophobic compounds (Oren and Chefetz, 2012) or plane deformation from guaiacyl units present in lignin molecules (Chen et al., 2015). The 1081 cm^{-1}C-O stretch band is common in polysaccharides and may indicate fresh plant residues in DOM (Soong et al., 2014). Its presence in DOM from char suggests that the carbonization process was incomplete.

The 1718 cm^{-1} band appears exclusively in DOM from the Stream and Litter. It may reflect protonated carboxylic groups or ketones, and can indicate the presence of weak acids that remain protonated (thus not bound to Al; González-Pérez et al., 2008). Bands that reflect aliphatic structures (2918–2850 cm^{-1}) appeared in greater evidence in Peat. The band at 1400 cm^{-1} was particularly expressed in Peat DOM, and may originate from aliphatic structures (Dick et al., 2003) or from Al complexed to carboxylate (Stevenson and Goh, 1971; Guan et al., 2006).

3.1.3. FTIR bands in leachates and trends in selective sorption

The FTIR spectra of leachates are presented for each column material (Fig. 2c–f). The nitrate band (1384 cm^{-1}) appeared in all spectra of leachates from the E-n columns (Fig. 2d). Spectra from E-h leachates showed bands at 1000, 835, and 700 cm^{-1} that are typical of AlO stretch (AlO_4) (Du et al., 2009). The minor kaolinite bands at 3550 and 3466 cm^{-1} that were present in both field-DOM samples (Stream and Peat) disappeared in spectra from the leachates, which indicates retention of this compound in the columns. These bands related to inorganic materials will not be considered further. The bands related to aliphatic CH (2950 and 2870 cm^{-1}) were ignored, because of their minor height and their location on the shoulder of the large broad peak in the 3450 cm^{-1} region (Fig. 2a). These aliphatic bands were present in the original DOM solution from Peat but did not appear in spectra from the leachates, suggesting retention of alkyl-C groups independently of column material. Retention of aliphatic C in the columns agrees with Ussiri and Johnson (2004) who found that hydrophobic fractions have higher alkyl-C and aromatic-C content, which was associated with relatively high MW and caused a lower solubility of DOM.

To explore the selectivity of DOM sorption, a PCA analysis was applied to selected FTIR bands. This selection is based on the presence of organic bands in both initial solutions and leachates and their potential interference with other bands, organic or inorganic. The selected organic bands are those at 1081, 1140, 1220, 1400, 1618 and 1718 cm^{-1}. From these, the 1081 cm^{-1} band is expressed as percentage of their sum. To correct for overlapping bands the 1140, 1220, 1400 and 1618 cm^{-1} bands are evaluated relative to the 1081 cm^{-1} band (i.e. 1140/1081, 1220/1081, 1400/1081, 1618/1081) (Ellerbrock and Kaiser, 2005), while the 1718 cm^{-1} will be expressed relative to the 1618 cm^{-1} (i.e. 1718/1618). The 1400 cm^{-1} band is not evaluated for leachates from E-n and E-h columns because its intensity is influenced by inorganic bands from $Al(OH)_3$ and nitrate (1384 cm^{-1}) (Fig. 2b,d,e). Therefore, the 1400 cm^{-1} band is excluded from PCA, and evaluated by comparing the average of leachates to the initial solution of corresponding DOM types (SI_Fig. 2d). In the following discussion, these six bands refer to these relative intensities.

Component 1 (Dim1) and component 2 (Dim2) together explained 75.4% of the variance of the samples (Fig. 3a). Dim1 shows positive loadings for the 1081 cm^{-1} band and negative loadings for phenolic groups (1220 cm^{-1}) and carboxylates (1618 cm^{-1}). The 1400 cm^{-1} band, that reflects carboxylic groups complexed to Al and is not included in PCA, positively correlates to 1618/1081 (r^2 = 0.92, data not shown). Dim1 thus separates carbohydrates (O-H; positive loadings) from phenolic and (complexed) carboxylic groups (negative loadings). Dim2 separates carboxylic acids and/or ketones (1718 cm^{-1}, positive loading) from hydrophobic aromatic compounds (1140 cm^{-1}, negative loading). The interpretation obtained from the loadings is supported by the grouping of samples in the scores (Fig. 3a). Dim1 separates Water and Stream with generally negative scores from Char, Peat and Litter with mostly positive scores, while Dim2 separates Char (negative) from Litter (positive). This suggests that Dim1 reflects soluble Al-DOM complexes, clearly indicated by the high negative scores of the Water leachates from the B columns (see also SI_Fig. 2), and that Al is mostly complexed to carboxylic and phenolic groups. While DOM from Litter, Peat and Char contains more intact OM rich in carbohydrates that is less soluble. Furthermore, Dim2 reflects that Char is additionally characterized by hydrophobic aromatic compounds, while Litter has a larger contribution from carboxylic acids (relative to the deprotonated COO^-), and Peat generally shows an intermediate composition between Char and Litter.

The distribution of samples in the scores figures is highlighted separately for the different column materials using arrows that connect DOM_in with leachates of the corresponding DOM (Fig. 3b-e). Leachates of B and E-h columns (and to a lesser extent also E-n) all show negative scores on Dim1, except for some Char samples (Fig. 3c-e). This indicates that B, E-n and E-h leachates, in particular B leachates after Water addition (Fig. 3e), contain more phenolic and (complexed) carboxylic groups. This is in agreement with the presence of reactive dissociated carboxylic groups in B-horizons, related to the accumulation of organometallic complexes in these horizons (González-Pérez et al., 2005), and with desorption of carboxylate products from the B-horizon (Jansen et al., 2004). Desorption of Al-DOM complexes from B-horizons explains the slightly negative scores of DOM_in from the Stream, considering that the Stream is sampled in the rainy season. During the rainy season precipitation causes lateral groundwater flow on top of the B-horizon in the catchment area of the stream (SI_Fig. 1). The negative scores of E-h and E-n leachates on Dim1 relates to a relatively larger portion of carboxylic complexes that remain soluble

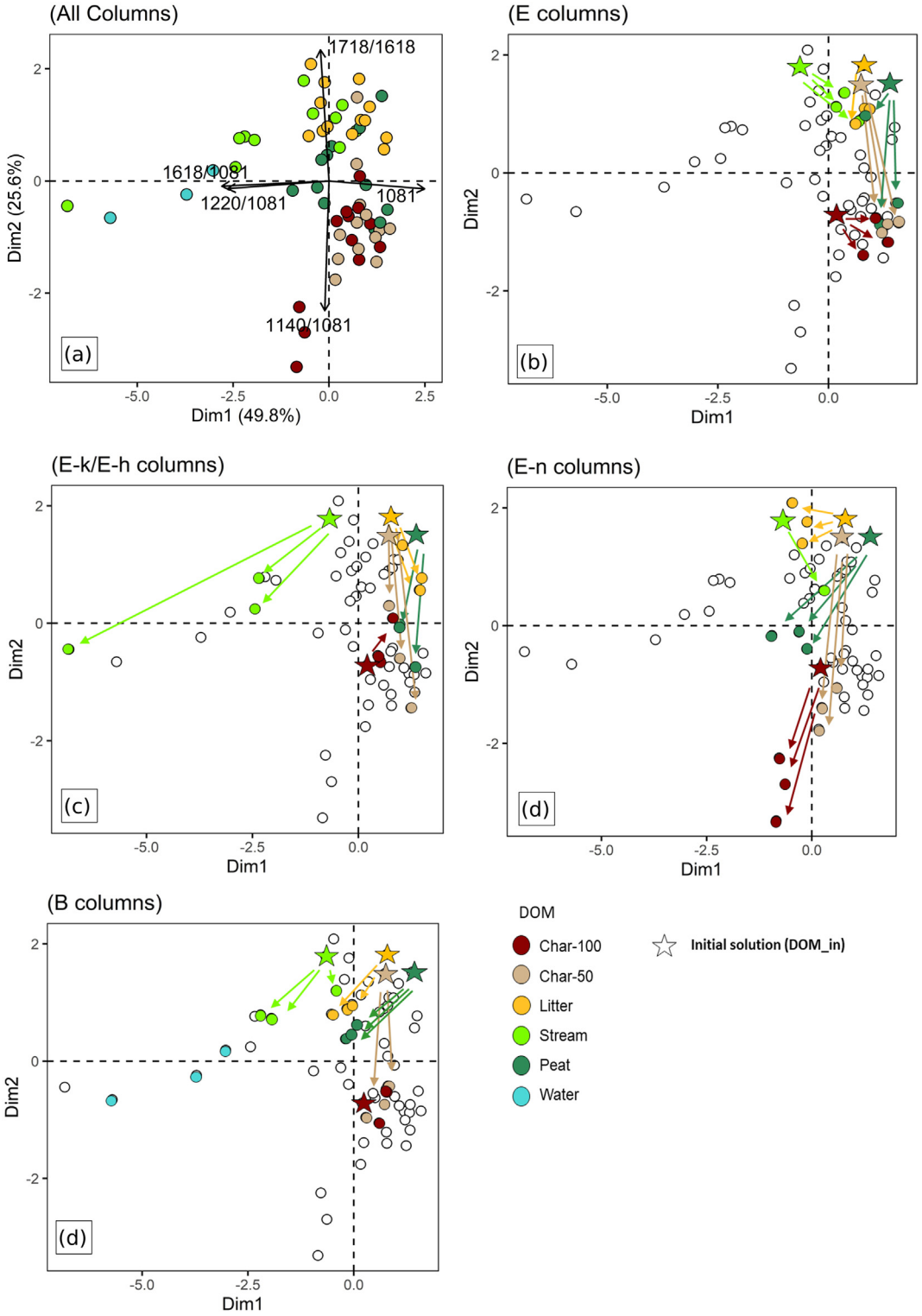

Fig. 3. Biplot with loadings and scores (a), and scores displayed individually for each column type (b-e) of Dim1 and Dim2 from PCA applied to selected FTIR spectral data. Symbols are colored according to DOM-type. The arrows connect DOM_in with its corresponding leachates.

compared to E columns with only solid or no Al (E-k and E; Jansen et al., 2003). Within the E columns the shifts on Dim1 were in the sequence E < E-k < E-n < E-h, which reflects an increase of soluble Al-DOM complexes in the leachates (Scheel et al., 2008). The relatively large and similar shifts on Dim1 for the B columns (except Char) and their directions towards the B Water leachates suggests that compositional changes in the B are largely due to desorption, and that this desorption is selective for phenolic and carboxylic groups. A slight shifts towards the positive side of Dim1 for some DOM types occurred in E and E-k columns, in particular Stream (Fig. 3b,c). This may reflect immobilization of the complexes due to saturation of DOM compounds with Al, which agrees with the fact that Stream already contained DOM-Al complexes.

All DOM types show a change towards negative scores on Dim2 from DOM_in to corresponding leachates reflecting retention of compounds

with ketones and/or carboxylic functional groups. The generally larger change towards the negative side of Dim2 suggests a larger effect of co-precipiation, i.e. retention without association to Al.

From all DOM types, Char samples showed the smallest change on Dim1 between initial solution and leachates in all columns, in particular Char-100 that showed virtually no change on both Dim1 and Dim2 (except for E-n). This suggests a relatively low capacity in both binding to Al and desorption. This low reactivity may be due to the relatively "fresh" char that composed the field samples, with characteristic decarboxylation and decarbonylation at high temperatures during the carbonization process, while the aromatic rings remain intact, which reduces organic reactive groups (Banik et al., 2018) and thus Al binding potential. In addition, it may reflect retention due to co-precipitation enhanced by the aromatic and hydrophobic properties of Char.

3.2. Py-GC/MS

3.2.1. Composition of the initial DOM solutions

Differences between DOM types in the abundance of groups of pyrolysis products generally agreed with their source (Table 2). There was a larger lignin contribution in DOM from Litter (8.2%) compared to other sources (0.0 to 1.1%). If plant material is the main source of DOM, this suggests a selective loss of lignin during its transport to the streams. This relative loss could be due to decomposition, (de)sorption, or an increasing contribution from microbial sources. Indeed, carbohydrates (13.3%) and N-containing compounds (10.8%) both have a relatively large contribution in DOM from Litter compared to other DOM types (0.3–8.4% and 6.7–10.2% for carbohydrates and N compounds, respectively), suggesting a predominant source from plant proteins, and/or plant-associated microorganism present in the litter (Kiikkilä et al., 2012). A higher relative abundance of N-containing compounds and carbohydrates is in agreement with the association of a hydrophilic fraction in DOM from Litter (Zang et al., 2021).

Polar compounds had clearly large contributions to DOM from the Stream, including benzofurans (6.2% compared to 1.7–3.2% in other DOM types), phenols (29% compared to 13.7–15.5%), and N-containing compounds (10.2%), reflecting the aqueous solubility of their source molecules (i.e. before pyrolysis; Schellekens et al., 2017).

The contribution from *n*-alkanes and *n*-alkenes was largest in DOM from Peat, together accounting for 23.7%, while for other DOM types this varied between 0.9 and 7.2%. These aliphatic pyrolysis products may be derived from leaf waxes and plant biopolymers such as cutan and suberan (Tegelaar et al., 1995) and are abundant in tropical peat (Schellekens et al., 2014). The relatively large contribution from aliphatic products in DOM from Peat is thus logically related to its source from peat water.

Benzenes was the dominant group in all DOM-types, and its contribution increases in the following sequence Litter < Peat < Stream < Char. Benzenes have many potential sources upon pyrolysis (e.g. lignin, charcoal, and proteins) their summed percentage may thus not be representative for sources or sorption processes in a variable sample set. DOM from Char includes the soluble products of the carbonization process of plant biomass, and indeed shows a larger contribution from PAHs (16.3 to 19.3%). Although PAHs may be a result of cyclization reactions during the pyrolysis process (Saiz-Jiménez, 1994), a large contribution is indicative for black carbon (Kaal et al., 2008).). In the Stream, PAHs (7.0%) may have a source from (partially degraded) burnt materials indicating the mobility of these compounds in the environment (Kim et al., 2004; Jaffé et al., 2013; Kaal et al., 2016).

Table 2
Relative abundance of groups of pyrolysis products (%TIC) of DOM_in for each DOM type.

Group	Stream	Litter	Peat	Char-50	Char-100
Benzenes	40.1	30.7	33.5	43.3	51.9
PAHs	7.00	5.02	12.6	16.3	19.3
Indenes	1.52	0.92	2.02	2.02	1.60
Benzofurans	6.19	1.66	2.42	3.23	2.51
N-compounds	10.2	10.8	6.65	9.34	7.11
Lignin phenols	1.09	8.15	0.00	0.07	0.00
Phenols	29.0	15.6	15.2	13.7	15.5
Carbohydrates	2.12	13.3	0.30	8.39	1.30
Triterpenes	0.06	0.07	2.44	0.23	0.31
Unidentified	0.00	4.84	0.13	0.00	0.00
Aliphatics	0.22	1.75	1.00	1.62	0.26
n-Alkanes	0.68	4.11	15.9	0.98	0.50
n-Alkenes	1.86	3.11	7.77	0.83	0.35

3.2.2. DOM composition in leachates and trends in selective molecular sorption

A PCA was performed to identify possible selective retention of organic compounds in the columns. The loadings (variables) and scores (samples) of the first two components are plotted in Figs. 4–5. Scores and loadings of the remaining components are given in SI_Tables 4 and 6. Loadings of PyDim1 (18.5% explained variance) indicate that products associated with charred material have positive loadings, in particular those with larger MW, including PAHs (PA10–20), and benzenes (B6–14) except benzenes with an acid functional group (B10–11). Products with high negative loadings on PyDim1, on the other hand, include low MW benzenes and N-containing products (N1–7, B1–2) (Fig. 4). This suggests that PyDim1 separates the products according to molecular size and aromaticity. PyDim2 (16.5%) shows positive loadings for products derived from biopolymers of plants (*n*-alkanes, *n*-alkenes, triterpenes, and lignin phenols) and microbes (N-containing compounds), and benzenes with alkyl side-chains (B3–9). Products with high negative loadings include aromatics with oxygenated or nitrogenated functional groups such as dibenzofuran (Bf4), benzonitrile (N7), benzoic acid (B10), and phenol (Ph1), or aromatics without alkyl side-chains such as benzene (B1), naphthalene (PA1) and fluorene (PA7). This suggests that PyDim2 separates products from more intact OM (positive loadings) vs. those derived from more processed OM (negative loadings).

The scores show a clear clustering according to DOM type in the PyDim1–2 projection (Fig. 5a). Samples from Peat and Char show positive scores on PyDim1, and are separated by PyDim2 with positive scores for Peat and negative ones for Char (with exception of the B leachates from Peat that have negative scores on PyDim1). Samples from Stream and Litter have negative scores on PyDim1, from which Litter samples have positive scores on PyDim2 and Stream samples negative scores. The Water leachates from the B columns have highest negative scores on PyDim1 and slightly negative scores on PyDim2. This division according to DOM type confirms the interpretation of the components obtained from the loadings. First, a larger contribution from plant- and microbial biopolymers in DOM from Litter and Peat (positive on PyDim2) is conform to their source. Their separation by PyDim1 reflects that Litter is richer in lignin-cellulose, indicated by lignin products (G and S) and levoglucosan (Ps5) that is indicative for cellulose (Pouwels et al., 1989). In tropical peat lignin is rapidly decomposed (Schellekens et al., 2014), which explains the relatively larger contribution from aliphatic and aromatic compounds in the Peat DOM. The negative scores on both components of Stream samples reflect that the stream contains more processed DOM, which was also indicated by the FTIR results by the presence of carboxylic functional groups, and is due to its natural riverine source.

The positive scores on PyDim1 of Peat and Char suggests that both contain DOM with relatively larger molecular size with relatively abundant PAHs. Comparing both DOM types, the Peat is more aliphatic as indicated by the positive loadings of aliphatic products (C:0, C:1, Al1–3) and the alkyl side-chains on the PAHs and benzenes. The grouping of the B leachates negative on PyDim1 with the highest negative scores for the Water samples agrees with the fact that the source of SOM from hydromorphic Bh-horizons is mainly from processed DOM instead of in-situ deposited root material (Bardy et al., 2008; Lopes-Mazzetto et al., 2018a), and with a more proteinaceous DOM desorbed from B columns (Merdy et al., 2021). A larger homogeneity of the Stream samples is indicated by the more compact clustering compared to other DOM types. This is also valid for the B leachates (in particular Water) compared to leachates from

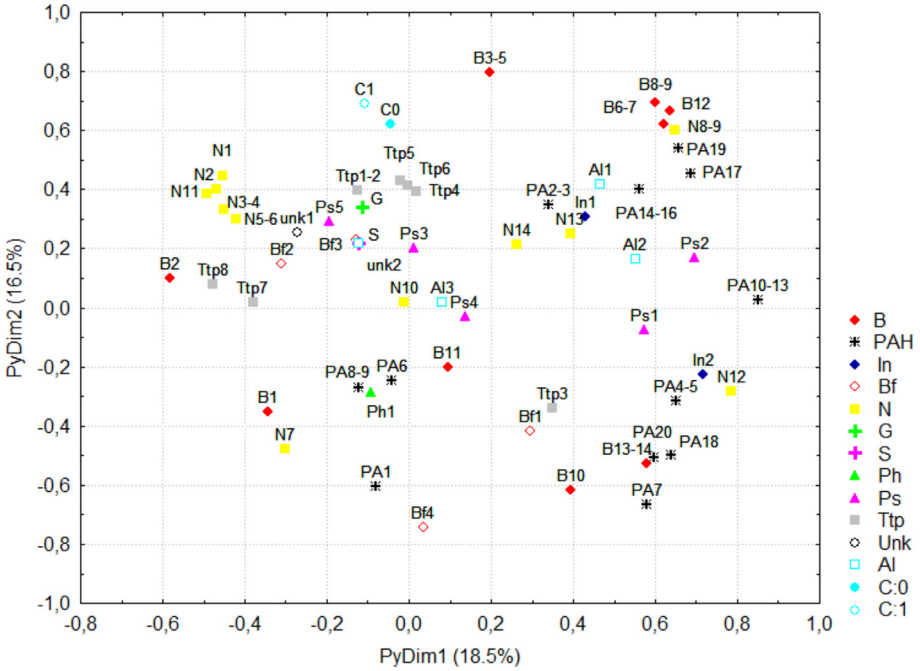

Fig. 4. Loadings for the PyDim1–PyDim2 projection from PCA applied to the Py-GC/MS data.

other columns, and may reflect a loss of molecular diversity during degradation of riverine DOM (O'Connor et al., 2012).

The sorption in the different column materials is indicated by arrows that connect DOM_in with its corresponding leachates (Fig. 5b–d). All DOM types show a converging trend towards the Water leachates (negative scores on PyDim1, neutral scores on PyDim2) after passing through the B columns (Fig. 5d). An explanation is that mainly desorption determined the composition of B leachates, with a minor role for the initial composition of DOM. The converging shift towards the Water leachates for all DOM types also reflects a relative retention of pyrolysis products from macromolecular structures (lignin, cellulose, black carbon) in the B columns, and is consistent with the fact that sorption of hydrophobic compounds causes the displacement of indigenous and hydrophilic substances (Kaiser et al., 1996).

In E, E-k and E-h columns the direction of the change is similar within each DOM type, but among the DOM types variation in this direction exists. For Char the direction of the change on PyDim1 after passing through E and E-k columns is similar to that of the B columns, indicating preferential retention of condensed aromatic structures. The similarity between column materials suggests that sorption without Al interaction is the main process causing retention of Char, and agrees with the lower contribution of reactive functional groups in Char as indicated by FTIR (Section 3.1.3).

For DOM types other than Char, DOM_in showed more negative scores on PyDim1 than corresponding leachates, except for E leachates from the Stream (equal scores). This reflects retention of material associated to low MW products in E and E-k columns. This interpretation is in line with the increasing length of the arrows in the sequence Stream<Litter<Peat, which is the same sequence as found for the clusters according to DOM type from negative to positive scores on PyDim1.

A more detailed comparison of the treatments shows that E-k/E-h leachates (Fig. 5c) consistently have more positive scores on PyDim1 than corresponding E leachates (Fig. 5b), which suggests that the selectivity of sorption due to binding with kaolin/ gibbsite is stronger.

For the Char samples the direction from DOM_in to leachates towards the negative side of PyDim1 suggests selective retention of polyaromatic macromolecules, such as was found for the B columns. This may indicate that also in E and E-k columns retention of DOM from Char occurred mainly without Al interaction. Sorption of Char thus had an opposed effect compared to sorption due to binding with Al in this experiment, which can be explained by the larger molecular size of recently produced charcoal, and contrarily the decrease in size that generally goes together with more processed OM. The other DOM types, however, showed an opposing direction on PyDim1 and diverging trend in E and E-k/E-h columns.

The diverging trend in E/Ek/Eh columns from the upper left corner towards negative scores on PyDim2 and positive scores on PyDim1 thus suggests that, while the preferential sorption in terms of functional groups was mostly similar for DOM types, the molecules that preferentially bind to Al differed between DOM types. This is mainly due to a varying contribution from N-containing compounds, with a low contribution in the Stream (no change on PyDim1), a more prominent role in the Peat (large shift on PyDim1) and moderate contribution in Litter. A prominent role for *n*-alkanes and *n*-alkenes was evident for all DOM types, since these compounds had high positive loadings on PyDim2 and negative loadings on PyDim1 (Fig. 4). A prominent role of N-compounds and aliphatics in soil OM binding properties is frequently reported for clay minerals (Lichtfouse et al., 1998; Grasset et al., 2009; Justi et al., 2018; Possinger et al., 2020; Yang et al., 2020). The opposing direction of the arrows for B columns and E-k/E-h columns on PyDim1 suggest that desorption and sorption involved the same molecules.

3.3. Selectivity of DOM sorption in the podzolization process

Our experiment indicates that during the percolation of DOM the soil behaves as a chromatographic column in which selective retention occurs (Kaiser and Guggenberger, 2000), but that this is not conform to a generic pattern and dependent on both DOM composition and the Al species in the soil. Both FTIR and Py-GC/MS indicated that DOM-Al interaction caused selective retention of DOM from biopolymers by a loss of cellulose (levoglucosan, 1081 cm^{-1}), cutin and suberin (aliphatic compounds, 2870 and 2950 cm^{-1}), lignin products and N-containing compounds in leachates from E, E-k and E-h columns. Precipitation without Al on the other hand was mainly associated to DOM from Char, and to a lesser extent Peat, and caused selective retention of aromatic hydrophobic material. The fact that precipitation was the dominant process for Char- and Peat-DOM, and the larger effect of binding with Al for Stream- and Litter-DOM agrees with the findings of Hagedorn et al. (2015), who found litter as the primary source of carbon that cheluviates in the soil and gives rise to the Bh-horizon of podzols. However, Char-DOM is hardly comparable to black carbon

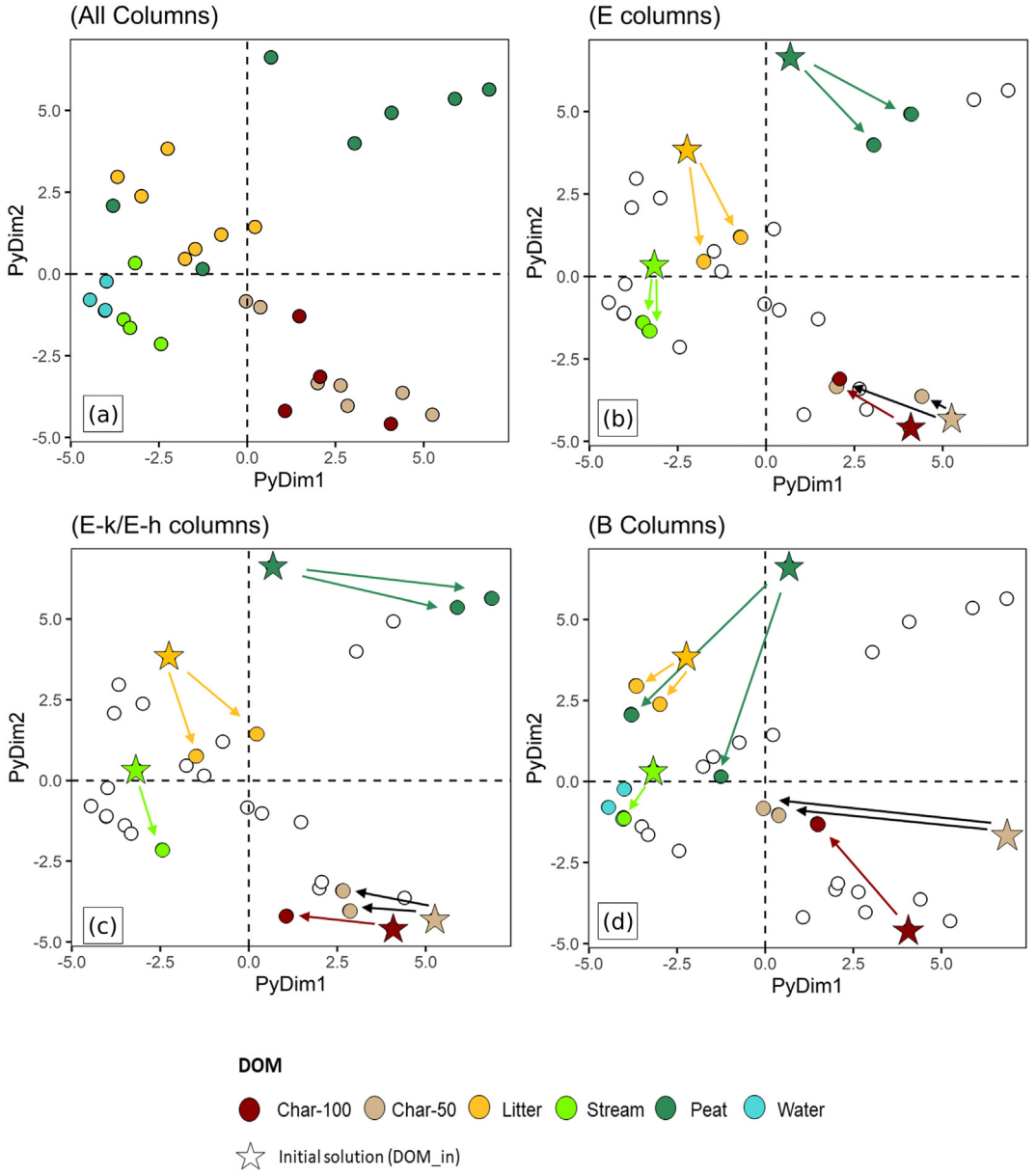

Fig. 5. Scores for the PyDim1–PyDim2 projection from PCA applied to the Py-GC/MS data, for all columns (a) and displayed individually for each column type (b-d). The arrows connect DOM_in with its corresponding leachates.

found in soil and streams from the field because it has not had enough time to form functional groups. Therefore, the importance of pyrogenic DOM in the formation of podzols (Hockaday et al., 2007; Eckmeier et al., 2010) cannot be judged. The composition of leachates after percolating through B columns resembled that of B SOM, independently of DOM type. This, together with the similarities between B Water leachates and the DOM from the Stream, reflects that desorption dominated in our experimental setting. These results suggests that in the tropical rainfall season the desorbed Bh OM would migrate from the soil and reach rivers or the ocean (Fritsch et al., 2009; Pérez et al., 2011), and demonstrates the importance of desorption of DOM from the podzol B-horizon in the Tropical Coastal Podzol area.

4. Conclusions

In the column experiment with E- and Bh-horizon material and DOM solutions representative for a Tropical Coastal Podzol environment, the molecular composition of DOM leachates was determined with FTIR and Py-GC/MS. The classical theory that DOM with carboxylic and phenolic functional groups preferentially binds to Al was confirmed by FTIR. Both FTIR and Py-CG/MS results suggested that retention of DOM was selective for hydrophobic macromolecular material. Independently of DOM composition, desorption from the B occurred, and this desorbed DOM was rich in low MW aromatic and N-containing products, rich in phenolic and carboxylic groups whether or not complexed to Al. The results from this column experiment suggest that DOM sorption with Al is selective but retention by non-polar forces was predominant. Furthermore, our results indicate that the amount and composition of SOM in Bh-horizons of this Tropical Coastal Podzol area are dynamic, and dependent on the input material, i.e. the composition of DOM. This dynamic character of sorption processes may have implications for 14-C dating of Bh-horizons, carbon sequestration in podzols, and the mobility of metals in the environment.

CRediT authorship contribution statement

Sara Ramos dos Santos: Methodology, Formal analysis, Investigation, Visualization, Writing - Original Draft. **Judith Schellekens:**

Conceptualization, Methodology, Supervision, Funding acquisition. **Wilson Tadeu Lopes da Silva:** Investigation, Resources. **Peter Buurman:** Conceptualization, Methodology. **Alexys Giorgia Friol Boim:** Methodology. **Pablo Vidal-Torrado:** Methodology, Investigation, Resources, Funding acquisition, Project administration. All co-authors contributed to Writing - Reviewing and Editing the original draft.

Declaration of competing interest

The authors declare that they have no known competing financial interests or personal relationships that could have appeared to influence the work reported in this paper.

Acknowledgements

This research was supported by the Fundação de Amparo à Pesquisa do Estado de São Paulo (FAPESP; grant number: 2018/07094-4), the National Council for Scientific and Technological Development (CNPq; grant number: 301818/2017-7), and the Flanders Research Foundation (FWO; grant number: 12ZY320N/SW). We thank Nivanda Maria de Moura Ruiz and Silviane Zanni Hubinger for the support in the laboratory. We thank three anonymous, in particular reviewers #2 and #3, for valubale comments.

References

Avneri-Katz, S., Young, R.B., McKenna, A.M., Chen, H., Corilo, Y.E., Polubesova, T., Borch, T., Chefetz, B., 2017. Adsorptive fractionation of dissolved organic matter (DOM) by mineral soil: macroscale approach and molecular insight. Org. Geochem. 103, 113–124. https://doi.org/10.1016/j.orggeochem.2016.11.004.

Banik, C., Lawrinenko, M., Bakshi, S., Laird, D.A., 2018. Impact of pyrolysis temperature and feedstock on surface charge and functional group chemistry of biochars. J. Environ. Qual. 47, 452–461. https://doi.org/10.2134/jeq2017.11.0432.

Bardy, M., Fritsch, E., Derenne, S., Allard, T., Do Nascimento, N.R., Bueno, G.T., 2008. Micromorphology and spectroscopic characteristics of organic matter in waterlogged podzols of the upper Amazon basin. Geoderma 145, 222–230. https://doi.org/10.1016/j.geoderma.2008.03.008.

Boča, A., Jacobson, A.R., Van Miegroet, H., 2020. Aspen soils retain more dissolved organic carbon than conifer soils in a sorption experiment. Front. For. Glob. Chang. 3, 594473. https://doi.org/10.3389/ffgc.2020.594473.

Buurman, P., Jongmans, A.G., 2005. Podzolisation and soil organic matter dynamics. Geoderma 125, 71–83. https://doi.org/10.1016/j.geoderma.2004.07.006.

Capriel, P., Beck, T., Borchert, H., Gronholz, J., Zachmann, G., 1995. Hydrophobicity of the organic matter in arable soils. Soil Biol. Biochem. 27, 1453–1458. https://doi.org/10.1016/0038-0717(95)00068-P.

Celi, L., Schnitzer, M., Nègre, M., 1997. Analysis of carboxyl groups in soil humic acids by a wet chemical method, Fourier transform infrared spectrometry and solution-state carbon-13 nuclear magnetic resonance. A comparative study. Soil Sci. 162, 189–197. https://doi.org/10.1097/00010694-199703000-00004.

Chen, L., Wang, X., Yang, H., Lu, Q., Li, D., Yang, Q., Chen, H., 2015. Study on pyrolysis behaviors of non-woody lignins with TG-FTIR and py-GC/MS. J. Anal. Appl. Pyrolysis 113, 499–507. https://doi.org/10.1016/j.jaap.2015.03.018.

Choe, E., van der Meer, F., Rossiter, D., van der Salm, C., Kim, K.W., 2010. An alternate method for fourier transform infrared (FTIR) spectroscopic determination of soil nitrate using derivative analysis and sample treatments. Water Air Soil Pollut. 206, 129–137. https://doi.org/10.1007/s11270-009-0091-z.

Core Team, 2015. R: A Language and Environment for Statistical Computing. R Foundation for Statistical Computing, Vienna, Austria.

De Coninck, F., 1980. Major mechanisms in formation of spodic horizons. Geoderma 24, 101–128. https://doi.org/10.1016/0016-7061(80)90038-5.

Dick, D.P., Santos, J.H.Z., Ferranti, E.M., 2003. Chemical characterization and infrared spectroscopy of soil organic matter from two southern brazilian soils. Rev. Bras. Cienc. Solo 27, 29–39. https://doi.org/10.1590/S0100-06832003000100004.

Du, X., Wang, Y., Su, X., Li, J., 2009. Influences of pH value on the microstructure and phase transformation of aluminum hydroxide. Powder Technol. 192, 40–46. https://doi.org/10.1016/j.powtec.2008.11.008.

Eckmeier, E., Egli, M., Schmidt, M.W.I., Schlumpf, N., Nötzli, M., Minikus-Stary, N., Hagedorn, F., 2010. Preservation of fire-derived carbon compounds and sorptive stabilisation promote the accumulation of organic matter in black soils of the southern Alps. Geoderma 159, 147–155. https://doi.org/10.1016/j.geoderma.2010.07.006.

Ellerbrock, R.H., Kaiser, M., 2005. Stability and composition of different soluble soil organic matter fractions-evidence from d13C and FTIR signatures. Geoderma 128, 28–37. https://doi.org/10.1016/j.geoderma.2004.12.025.

Fritsch, E., Allard, Th., Benedetti, M.F., Bardy, M., Do Nascimento, N.R., Li, Y., Calas, G., 2009. Organic complexation and translocation of ferric iron in podzols of the Negro River watershed. Separation of secondary fe species from Al species. Geochim. Cosmochim. Acta 73, 1813–1825. https://doi.org/10.1016/j.gca.2009.01.008.

Gomes, F.H., Vidal-Torrado, P., Macías, F., Souza Júnior, V.S., Perez, X.L.O., 2007. Solos sob vegetação de Restinga na ilha do Cardoso (SP): II - mineralogia das frações silte e argila. Rev. Bras. Ciênc. Solo 31, 1581–1589. https://doi.org/10.1590/S0100-06832007000600034.

González-Pérez, M., Vidal-Torrado, P., Colnago, L.A., Martin-Neto, L., Otero, X.L., Milori, D.M.B.P., Gomes, F.H., 2008. 13C NMR and FTIR spectroscopy characterization of humic acids in spodosols under tropical rain forest in southeastern Brazil. Geoderma 146, 425–433. https://doi.org/10.1016/j.geoderma.2008.06.018.

Grasset, L., Martinod, J., Plante, A.F., Amblès, A., Chenu, C., Righi, D., 2009. Nature and origin of lipids in clay size fraction of a cultivated soil as revealed using preparative thermochemolysis. Org. Geochem. 40, 70–78. https://doi.org/10.1016/j.orggeochem.2008.09.004.

Guan, X.H., Shang, C., Chen, G.H., 2006. ATR-FTIR investigation of the role of phenolic groups in the interaction of some NOM mode compounds with aluminum hydroxide. Chemosphere 65, 2074–2081. https://doi.org/10.1016/j.chemosphere.2006.06.048.

Guggenberger, G., Kaiser, K., 2003. Dissolved organic matter in soil: challenging the paradigm of sorptive preservation. Geoderma 113, 293–310. https://doi.org/10.1016/S0016-7061(02)00366-X.

Hagedorn, F., Bruderhofer, N., Ferrari, A., Niklaus, P.A., 2015. Tracking litter-derived dissolved organic matter along a soil chronosequence using 14C imaging: biodegradation, physico-chemical retention or preferential flow? Soil Biol. Biochem. 88, 333–343. https://doi.org/10.1016/j.soilbio.2015.06.014.

Harris, W.G., Rischar, C.A., 2012. Factors related to bh-horizon depth for artificial and natural E-bh sequences. Geoderma 189–190, 502–507. https://doi.org/10.1016/j.geoderma.2012.06.020.

Hockaday, W.C., Grannas, A.M., Kim, S., Hatcher, P.G., 2007. The transformation and mobility of charcoal in a fire-impacted watershed. Geochim. Cosmochim. Acta 71, 3432–3445. https://doi.org/10.1016/j.gca.2007.02.023.

Jaffé, R., Ding, Y., Niggeman, J., Vähätalo, A.V., Stubbins, A., Spencer, R.M., Campbell, J., Dittmar, T., 2013. Global charcoal mobilization from soils via dissolution and riverine transport to oceans. Science 340, 345–347. https://doi.org/10.1126/science.1231476.

Jansen, B., Nierop, K.G.J., Verstraten, J.M., 2003. Mobility of Fe(II), Fe(III) and Al in acidic forest soils mediated by dissolved organic matter: influence of solution pH and metal/organic carbon ratios. Geoderma 113, 323–340. https://doi.org/10.1016/S0016-7061(02)00368-3.

Jansen, B., Nierop, K.G.J., Verstraten, J.M., 2004. Mobilization of dissolved organic matter, aluminium and iron in podzol eluvial horizons as affected by formation of metal–organic complexes and interactions with solid soil material. Eur. J. Soil Sci. 55, 287–297. https://doi.org/10.1111/j.1365-2389.2004.00598.x.

Jansen, B., Nierop, K.G.J., Verstraten, M.J., 2005. Mechanisms controlling the mobility of dissolved organic matter, aluminium and iron in podzol B horizons. Eur. J. Soil Sci. 56, 537–550. https://doi.org/10.1111/j.1365-2389.2004.00686.x.

Justi, M., Schellekens, J., De Camargo, P.B., Vidal-Torrado, P., 2018. Long-term degradation effect on the molecular composition of black carbon in brazilian cerrado soils. Org. Geochem. 113, 196–209. https://doi.org/10.1016/j.orggeochem.2017.06.002.

Kaal, J., Brodowski, S., Baldock, J.A., Nierop, K.G.K., Cortizas, A.M., 2008. Characterisation of aged black carbon using pyrolysis-GC/MS, thermally assisted hydrolysis and methylation (THM), direct and cross-polarisation 13C nuclear magnetic resonance (DP/CP NMR) and the benzenepolycarboxylic acid (BPCA) method. Org. Geochem. 39, 1415–1426. https://doi.org/10.1016/j.orggeochem.2008.06.011.

Kaal, J., Wagner, S., Jaffé, R., 2016. Molecular properties of ultrafiltered dissolved organic matter and dissolved black carbon in headwater streams as determined by pyrolysis-GC-MS. J. Anal. Appl. Pyrolysis 118, 181–191. https://doi.org/10.1016/j.jaap.2016.02.003.

Kaiser, K., Guggenberger, G., 2000. The role of DOM sorption to mineral surfaces in the preservation of organic matter in soils. Org. Geochem. 31, 711–725. https://doi.org/10.1016/S0146-6380(00)00046-2.

Kaiser, K., Guggenberger, G., Zech, W., 1996. Sorption of DOM and DOM fractions to forest soils. Geoderma 74, 281–303. https://doi.org/10.1016/S0016-7061(96)00071-7.

Kaiser, K., Guggenberger, G., Haumaier, L., Zech, W., 1997. Dissolved organic matter sorption on subsoils and minerals studied by 13C-NMR and DRIFT spectroscopy. Eur. J. Soil Sci. 48, 301–310. https://doi.org/10.1111/j.1365-2389.1997.tb00550.x.

Kalbitz, K., Schwesig, D., Rethemeyer, J., Matzner, E., 2005. Stabilization of dissolved organic matter by sorption to the mineral soil. Soil Biol. Biochem. 37, 1319–1331. https://doi.org/10.1016/j.soilbio.2004.11.028.

Kiikkilä, O., Kitunen, V., Spetz, P., Smolander, A., 2012. Characterization of dissolved organic matter in decomposing Norway spruce and silver birch litter. Eur. J. Soil Sci. 63, 476–486. https://doi.org/10.1111/j.1365-2389.2012.01457.x.

Kim, S., Kaplan, L.A., Benner, R., Hatcher, P.G., 2004. Hydrogen deficient molecules in natural riverine water samples - evidence for the existence of black carbon in DOM. Mar. Chem. 92, 225–234. https://doi.org/10.1016/j.marchem.2004.06.042.

Kothawala, D.N., Roehm, C., Blodau, C., Moore, T.R., 2012. Selective adsorption of dissolved organic matter to mineral soils. Geoderma 189–190, 334–342. https://doi.org/10.1016/j.geoderma.2012.07.001.

Leão, Z.M.A.N., Dominguez, J.M.L., 2000. Tropical coast of Brazil. Mar. Pollut. Bull. 41, 112–122. https://doi.org/10.1016/S0025-326X(00)00105-3.

Lichtfouse, E., Lebond, C., Da Silva, M., Behar, F., 1998. Occurrence of biomarkers and straight-chain biopolymers in humin: implication for the origin of soil organic matter. Naturwissenschaften 85, 497–501. https://doi.org/10.1007/s001140050538.

Lopes-Mazzetto, J.M., Schellekens, J., Vidal-Torrado, P., Buurman, P., 2018a. Impact of drainage and soil hydrology on sources and degradation of organic matter in tropical coastal podzols. Geoderma 330, 79–90. https://doi.org/10.1016/j.geoderma.2018.05.015.

Lopes-Mazzetto, J.M., Buurman, P., Schellekens, J., Martinez, P.H.R.M., Vidal-Torrado, P., 2018b. Soil morphology related to hydrology and degradation in tropical coastal podzols (SE Brazil). Catena 162, 1–13. https://doi.org/10.1016/j.catena.2017.11.007.

Ma, H., Allen, H.E., Yin, Y., 2001. Characterization of isolated fractions of dissolved organic matter from natural waters and a wastewater effluent. Water Res. 35, 985–996. https://doi.org/10.1016/S0043-1354(00)00350-X.

Martin, A.E., Reeve, R., 1961. Chemical studies of podzolic illuvial horizons. IV the flocculation of humus by aluminium. J. Soil Sci. 11, 369–381. https://doi.org/10.1111/j.1365-2389.1960.tb01091.x.

Martinez, P., Buurman, P., Lopes-Mazzetto, J.M., César, P., Giannini, F., Schellekens, J., Vidal-Torrado, P., 2018. Geomorphology geomorphological control on podzolisation – an example from a tropical barrier island. Geomorphology 309, 86–97. https://doi.org/10.1016/j.geomorph.2018.02.030.

Merdy, P., Lucas, Y., Coulomb, B., Melfi, A.J., Montes, C.R., 2021. Soil organic carbon mobility in equatorial podzols: soil column experiments. Soil 7, 585–594. https://doi.org/10.5194/soil-7-585-2021 2021.

Mikutta, R., Mikutta, C., Kalbitz, K., Scheel, T., Kaiser, K., Jahn, R., 2007. Biodegradation of forest floor organic matter bound to minerals via different binding mechanisms. Geochim. Cosmochim. Acta 71, 2569–2590. https://doi.org/10.1016/j.gca.2007.03.002.

Nebbioso, A., Piccolo, A., 2013. Molecular characterization of dissolved organic matter (DOM): a critical review. Anal. Bioanal. Chem. 405, 109–124. https://doi.org/10.1007/s00216-012-6363-2.

Nierop, K.G.J., Jansen, B., Verstraten, J.M., 2002. Dissolved organic matter, aluminium and iron interactions: precipitation induced by metal/carbon ratio, pH and competition. Sci. Total Environ. 300, 201–211. https://doi.org/10.1016/S0048-9697(02)00254-1.

O'Connor, J.A., Lu, K., Guo, L., Rosenheim, B.E., Liu, Z., 2012. Composition and lability of riverine dissolved organic matter: insights from thermal slicing ramped pyrolysis GC/MS, amino acid, and stable isotope analyses. Org. Geochem. 149, 104100.

Oren, A., Chefetz, B., 2012. Sorptive and desorptive fractionation of dissolved organic matter by mineral soil matrices. J. Environ. Qual. 41, 526–533. https://doi.org/10.2134/jeq2011.0362.

Pavinato, P.S., Merlin, A., Rosolem, C.A., 2018. Organic compounds from plant extracts and their effect on soil phosphorus availability. Pesq. Agrop. Brasileira 43, 1379–1388. https://doi.org/10.1590/S0100-204X2008001000017.

Pérez, M.A.P., Moreira-Turcq, P., Gallard, H., Allard, H., Benedetti, M.F., 2011. Dissolved organic matter dynamic in the Amazon basin: sorption by mineral surfaces. Chem. Geol. 286, 158–168. https://doi.org/10.1016/j.chemgeo.2011.05.004.

Phinichka, N., Kaenthong, S., 2017. Regenerated cellulose from high alpha cellulose pulp of steam-exploded sugarcane bagasse. Mater. Res. Technol. 7, 55–65. https://doi.org/10.1016/j.jmrt.2017.04.003.

Possinger, A.R., Zachman, M.J., Enders, A., Levin, B.D.A., Muller, D.A., Kourkoutis, L.F., Lehmann, J., 2020. Organo–organic and organo–mineral interfaces in soil at the nanometer scale. Nat. Commun. 11, 6103. https://doi.org/10.1038/s41467-020-19792-9.

Pouwels, A.D., Eijkel, G.B., Boon, J.J., 1989. Curie-point pyrolysis high-resolution gas chromatography/mass spectrometry of microcrystalline cellulose. J. Anal. Appl. Pyrolysis 14, 237–280. https://doi.org/10.1016/0165-2370(89)80003-8.

Refaey, Y., Jansen, B., El-Shater, A., El-Haddad, A., Kalbitz, K., 2014. The role of dissolved organic matter in adsorbing heavy metals in clay-rich soils. Vadose Zone J. 13, 1–12. https://doi.org/10.2136/vzj2014.01.0009 vzj2014.01.0009.

Saiz-Jiménez, C., 1994. Production of alkylbenzenes and alkylnaphthalenes upon pyrolysis of unsaturated fatty acids. Naturwissenschaften 81, 451–453.

Scheel, T., Dörfler, C., Kalbitz, K., 2007. Precipitation of dissolved organic matter by Al stabilizes C in acidic forest soils. Soil Sci. Soc. Am. J. 71, 64–74. https://doi.org/10.2136/sssaj2006.0111.

Scheel, T., Haumaier, L., Ellerbrock, R.H., Rühlmann, J., Kalbitz, K., 2008. Properties of organic matter precipitated from acidic forest soil solutions. Org. Geochem. 39, 1439–1453. https://doi.org/10.1016/j.orggeochem.2008.06.007.

Schellekens, J., Horák-Terra, I., Buurman, P., Silva, A.C., Vidal-Torrado, P., 2014. Holocene vegetation and fire dynamics in Central-Eastern Brazil: molecular records from the Pau de fruta peatland. Org. Geochem. 77, 32–42. https://doi.org/10.1016/j.orggeochem.2014.08.011.

Schellekens, J., Buurman, P., Kalbitz, K., Van Zomeren, A., Vidal-Torrado, P., Cerli, C., Comans, R.N.J., 2017. Molecular features of humic acids and fulvic acids from contrasting environments. Environ. Sci. Technol. 51, 1330–1339. https://doi.org/10.1021/acs.est.6b03925.

Scott, E., Rothstein, D., 2014. The dynamic exchange of dissolved organic matter percolating through six diverse soils. Soil Biol. Biochem. 69, 83–92. https://doi.org/10.1016/j.soilbio.2013.10.052.

Soong, J.L., Calderón, F.J., Betzen, J., Cotrufo, M.F., 2014. Quantification and FTIR characterization of dissolved organic carbon and total dissolved nitrogen leached from litter: a comparison of methods across litter types. Plant Soil 385, 125–137. https://doi.org/10.1007/s11104-014-2232-4.

Stevenson, F.J., Goh, K.M., 1971. Infrared spectra of humic acids and related substances. Geochim. Cosmochim. Acta 35, 471–483. https://doi.org/10.1016/0016-7037(71)90044-5.

Sutherland, R.A., 1998. Loss-on-ignition estimates of organic matter and relationships to organic carbon in fluvial bed sediments. Hydrobiologia 389, 153–167. https://doi.org/10.1023/A:1003570219018.

Tegelaar, E.W., Hollman, G., van der Vegt, P., de Leeuw, J.W., Holloway, P.J., 1995. Chemical characterization of the peridermtissue of some angiospermspecies: recognition of an insoluble, non-hydrolyzable, aliphatic biomacromolecule (Suberan). Org. Geochem. 23, 239–251.

Ussiri, D.A.N., Johnson, C.E., 2004. Sorption of organic carbon fractions by spodosol mineral horizons. Soil Sci. Soc. Am. J. 68, 253–262. https://doi.org/10.2136/sssaj2004.2530.

Vaculíková, L., Plevová, E., Vallová, S., Koutník, I., 2011. Characterization and differentiation of kaolinites from selected czech deposits using infrared spectroscopy and differential thermal analysis. Acta Geodyn. Geomater. 8, 59–67.

Yang, S., Jansen, B., Absalah, S., Kalbitz, K., Cammeraat, E., 2020. Selective stabilization of soil fatty acids related to their carbon chain length and presence of double bonds in the peruvian Andes. Geoderma 373, 114414. https://doi.org/10.1016/j.geoderma.2020.114414.

Zhang, X., Wang, Y., Wen, J., Zhang, Y., Su, S., Wen, Y., Yan, M., Bai, L., Wu, C., Zeng, X., 2021. The C/N ratio and phenolic groups of exogenous dissolved organic matter together as an indicator for evaluating the stability of mineral-organic associations in red soil. J. Soils Sediments 21, 821–831. https://doi.org/10.1007/s11368-020-02874-y.

Zysset, M., Berggren, D., 2001. Retention and release of dissolved organic matter in podzol B horizons. Eur. J. Soil Sci. 52, 409–421. https://doi.org/10.1046/j.1365-2389.2001.00399.x.